Bulletin of the Earthquake
Research Institute
Vol. 47 (1969), pp. 849-862

38. *Numerical Experiments for Tsunamis caused by Moving Deformations of the Sea Bottom.*

By Isamu Aida,

Earthquake Research Institute.

(Read May 27, 1969.—Received July 30, 1969.)

Abstract

Numerical experiments have been performed to investigate the nature of tsunami generated by the progressive deformation of a sea bottom. The deformation is assumed as follows: The initial time of the vertical movement delays successively in the x direction and the final elevation of a bottom is expressed by the formula, $\exp(-r^2/a^2)$.

The directivity coefficient, which is defined by the ratio between the heights of waves radiated in opposite directions, is obtained with respect to the horizontal speed of the bottom deformation. An experiment for a sloping bottom shows clearly that the directivity becomes still stronger by the effect of the decreasing depth in the direction of the movement of deformation.

1. Introduction

Recent studies for the source mechanism of an earthquake have confirmed the fact that the dislocation progressed along a focal plane [*Hirasawa*, 1965 and *Ben-Menahem and Toksöz*, 1962, etc.]. Therefore, it is plausible that the sea bottom deformation caused by a shallow earthquake under the sea bed also moves horizontally with a finite speed.

The nature of a tsunami caused by a moving bottom deformation has been studied theoretically for a one-dimensional model by *Homma* [1950, 1952a] and *Ichiye* [1950, 1951] and for a two-dimensional model by *Homma* [1952b]. However, the study for a two-dimensional model has been made with respect to the wave front only, and the wave amplitude has not been discussed.

It is a very important but difficult problem to determine the moving direction and speed of a bottom deformation from observed data of a tsunami. As a first step to approach this problem, the nature of tsunami generated by a moving source is investigated for a two dimensional model by means of a numerical experiment.

2. Method of numerical experiment

The x and y axes are put on the water surface. If the vertical displacement of a bottom and the water elevation relative to a still water level are denoted by η and ζ, the basic equations under the long wave approximation are

$$\left.\begin{aligned} &\frac{\partial}{\partial t}(\zeta-\eta)=-\frac{\partial q_x}{\partial x}-\frac{\partial q_y}{\partial y},\\ &\frac{\partial q_x}{\partial t}=-g(h-\eta+\zeta)\frac{\partial \zeta}{\partial x},\\ \text{and}\quad &\frac{\partial q_y}{\partial t}=-g(h-\eta+\zeta)\frac{\partial \zeta}{\partial y}, \end{aligned}\right\}$$

where q_x and q_y are the x and y components of the transport integrated from the surface to the bottom, and g is the acceleration of gravity. These equations are rewritten in a finite difference form and a numerical computation is carried out by an explicit method previously adopted by the writer [1969] in a numerical experiment for a tsunami propagation.

30×30 grid points for the computation are taken on rectangular meshes. The relation of progressive long waves between the water elevation and the transport is introduced as the boundary condition at the outer limit of the computing grids. Fig. 1 shows the computing grid scheme, in which the deformed area of sea bottom is inside a circle, approximated by the winding thick line.

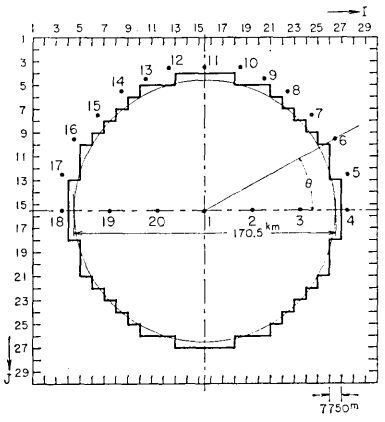

Fig. 1. Grid scheme of the computation. Numbered points are the places where water elevations are printed.

Time step $\Delta\tau$ is 0.05 minutes and the water elevation is printed in every 0.25 minutes at the points shown by numbered, closed circles in the figure.

3. Bottom elevated with a finite speed

This kind of tsunami generation problem was treated by *Takahasi* [1942, 1945] and *Nakamura* [1953]. In this section, the reliability of the method of a numerical experiment is examined by comparison with the analytical solution according to *Kajiura's* method [1966].

At first, a case in which the sea bottom is elevated uniformly in a

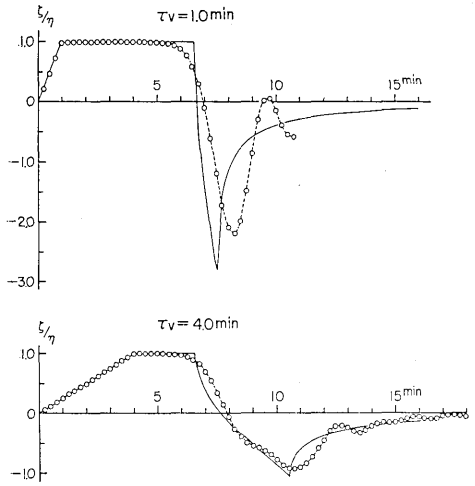

Fig. 2. Wave form at the center of a cylindrical deformed area. Open circles show the present result and solid lines show the analytical one. τ_v is a duration time of deformation.

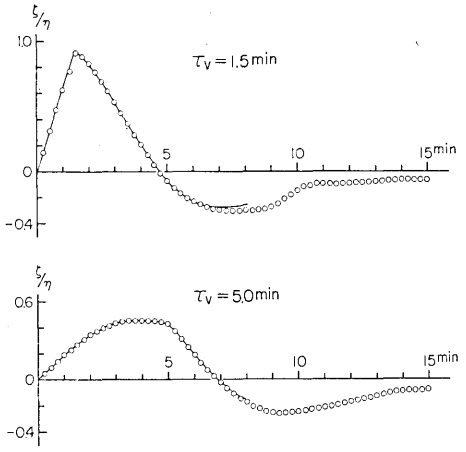

Fig. 3. Wave form at the center of the deformed area in which the shape of bottom deformation is expressed by $\exp(-r^2/a^2)$. Open circles show the present result and solid lines show the analytical one.

circular area with a constant speed is considered. In this case, the grid interval 5 km, the diameter of deformed area 110 km, the elevation of bottom 1 m and the water depth 2000 m were assumed. The computed sea surface elevation at the center of the deformed area is shown by open circles in Fig. 2. In the upper figure, the duration time of bottom deformation, τ_v, is assigned to 1 min and, in the lower figure, 4 min. A solid line in the figure is the analytical result with the same parameters. In a numerical experiment, the wave components of relatively short period are filtered out by the coarsness of the grid mesh, so that, in the case of $\tau_v=1$ min, the computed result is considerably different from the analytical one in the neighborhood of a sharp trough. However, in the case of $\tau_v=4$ min, both results show a fairly good coincidence on the whole.

In the other model examined, the bottom elevation η is expressed by $\exp(-r^2/a^2)$, where r is the distance from the center of the deformed area with a constant. The deformed area is assumed to be terminated at a distance of 85.25 km from the center, because the deformation beyond this distance is less than 1/20 of the one at the center. The results are shown by open circles in Fig. 3 with respect to $\tau_v=1.5$ and 5.0 min, which are in very good agreement with the analytical results shown by solid lines.

Judging from the above results, a high accuracy can be expected in the case when the shape of the final deformation of a sea bottom is

smooth. Consequently, our following experiments will be developed under the conditions; $\eta=\exp(-r^2/a^2)$ and $\tau_v=1.5$ min.

4. Deformation moved horizontally in the sea bottom

4a. Assumption of a bottom deformation

The plane figure of a model is a circle with a diameter d. Taking the x axis on a diameter, the origin is put at the left side intersection of the x axis and a circle. The deformation is supposed to move toward the positive x direction from the origin. τ_h is the time interval for the bottom deformation to move from the origin to the point, $x=d$, and τ_v is the time duration of vertical deformation similar to the one in the preceding section. The horizontal speed v_h is d/τ_h. Assuming the deformation started from the origin at $t=0$, the initial time t_i of the deformation at x is $t_i=x/v_h=(x/d)\tau_h$.

The vertical elevation of a sea bottom at the coordinate (x, y) at time t is assumed as follows;

$$\eta=0, \quad \text{for} \quad t<t_i,$$

$$\eta=\{(t-t_i)/\tau_v\}\exp(-r^2/a^2), \quad \text{for} \quad t_i+\tau_v>t\geq t_i,$$

and

$$\eta=\exp(-r^2/a^2), \quad \text{for} \quad t\geq t_i+\tau_v,$$

where

$$r^2=(x-d/2)^2+y^2.$$

The present experiment is carried out under the condition; $a=50$ km, the water depth 4000 m, $\tau_v=1.5$ min and the parameter τ_h is chosen to be 0, 1, 2, 3 and 5 min.

4b. Wave form generated

As an example for $\tau_h=3$ min, profiles of sea surface elevation inside the deformed area along the x axis are displayed in time sequence in Fig. 4. As the bottom deformation moves from left to right, the surface elevation also progresses toward right. In this example, when the bottom deformation at the center of the area is just completed at $t=3$ min, the uplift of bottom is just beginning at the right end of area and the water surface is not disturbed yet. Although the bottom deformation is completed in the whole area at $t=4.5$ min, as shown by a broken line, η_m, the maximum elevation of water had already moved toward the moving direction, as seen in the profile at $t=4.0$ min. When the deformation does not move horizontally, the clear trough appears at the center of area, following the first large crest. In the present case, the trough also moves toward right as seen in the profiles at 6, 8 and 10 min, and after that, it progresses separately to both sides as seen in the profiles at 12 and 14 min.

The generated wave forms shown in Fig. 5 are those at various points on the circumference of deformed area in Fig. 1, where τ_h is 3 min and the progressing direction of deformation is shown by an arrow. The wave form for No. 18 is superposed by a broken line on the form for No. 4, in the right end figure. It is apparent that the waves radiated in the moving direction is larger in amplitude and shorter in period than in the opposite direction.

The time when the waves appear initially at each point from No. 18 to No. 4 is successively delayed with the movement of bottom deformation, but the arrival time of the crest does not vary so much. The points from No. 4 to No. 18 are expressed by the azimuth θ measured counterclockwise from the positive x direction and the arrival times of the wave-front and the first crest are shown in Fig. 6 with respect to the azimuth θ.

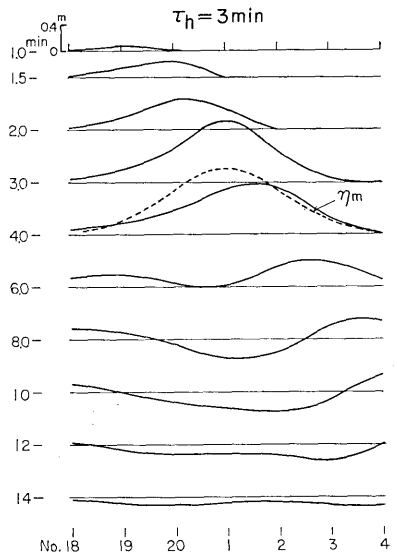

Fig. 4. Profiles of sea surface elevation over the deformed area moving horizontally. τ_h is the horizontal moving time of a bottom deformation. η_m is the final shape of a bottom deformation.

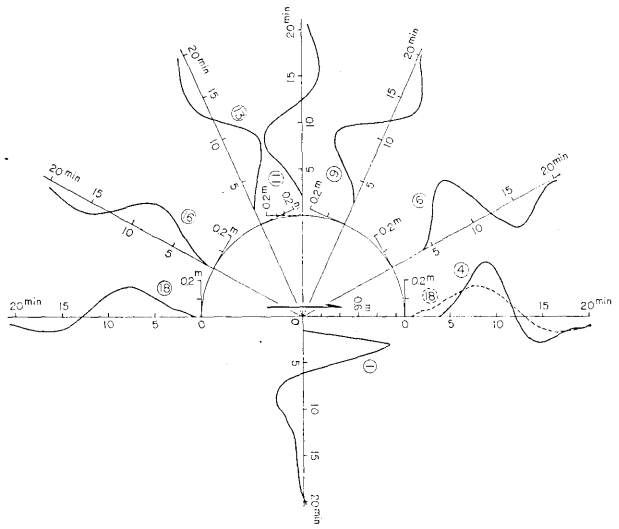

Fig. 5. Wave form obtained at the circumference of deformed area. The deformation moves in the direction shown by an arrow.

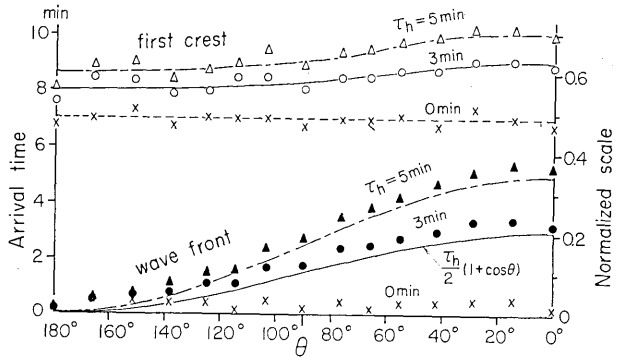

Fig. 6. Arrival times of a front and a crest of wave radiated toward the azimuth θ measured counterclockwise from the moving direction of deformation.

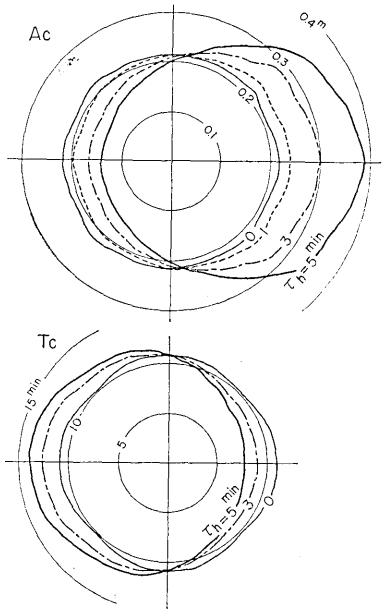

Fig. 7. Radiation patterns with respect to the amplitude and the half period.

Since the points where the water elevation is computed are about one grid interval outside the margin of circular area, the arrival time of wave-front should be 0.65 min in the case of $\tau_h=0$. In practice, however, a scattering of values is seen, which may be attributed to the non-uniformity of radial distance due to the approximation by rectangular mesh and to the uncertainty due to a gradual rise of initial motion of waves.

The beginning time of the bottom deformation on the margin of the deformed area is expressed by the form $t_b=(\tau_h/2)(1+\cos\theta)$ and, in the case of $\tau_h=3$ and 5 min, it is seen that the arrival of wave-front is the propagation time for one grid interval behind the time t_b. The changes of the arrival time of crest with respect to the azimuth θ is much smaller than that of the wave-front, and the time difference between $\theta=0°$ and 180° is about 1 to 1.5 min. Consequently, it is remarkable that the time between the wave-front and the crest changes considerably with respect to the azimuth θ.

The radiation patterns of the amplitude and the period of waves in every direction are shown in Fig. 7. A_c is the pattern for an amplitude

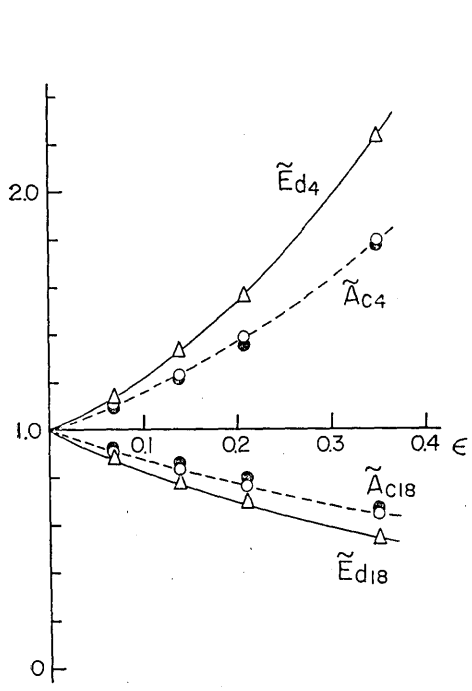

Fig. 8. Amplitudes of a crest and a trough, A_c and A_t, and the energy, E_d, of waves radiated in the progressing direction and in the opposite direction, which are shown by the relative value to the one of $\varepsilon=0$. The abscissa ε is $\sqrt{gh}/v_h$, where $\sqrt{gh}$ is a long wave velocity and $v_h=d/\tau_h$.

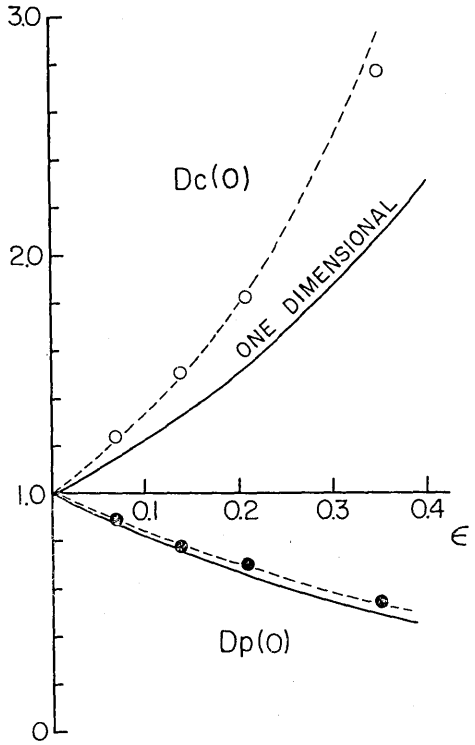

Fig. 9. Directivity coefficients of a crest amplitude and a half period, $D_c(0)$ and $D_p(0)$, which are defined by the ratio of the value of the wave radiated in opposite directions.

of crest and T_c the one for the duration time of positive half wave, so-called the half period. Taking into account the fluctuation of the pattern for $\tau_h=0$ min, the error in A_c falls in the range of $\pm 2.5\%$. The deviation in T_c is rather large, being $\pm 3.5\%$.

4c. Directivity coefficient

As seen clearly from the radiation pattern of the wave, a remarkable difference between the waves radiated toward the moving direction and those toward the opposite direction is recognized in the amplitude and period.

The variations of the amplitudes of a crest and a trough and of the wave energy transmitted through a unit width on a circle are examined with respect to the speed of a bottom deformation, as shown in Fig. 8. The speed of a bottom deformation is expressed in the term $\varepsilon=\sqrt{gh}/v_h$, where $\sqrt{gh}$ is the long-wave velocity and $v_h=d/\tau_h$. As the water depth

is 4000 m, the relation between the duration time of the horizontal movement, τ_h, and ε is tabulated as follows.

Table 1.

τ_h (min)	1.0	2.0	3.0	5.0
ε	0.0697	0.139	0.209	0.348

In Fig. 8, the amplitude of crest and trough and the wave energy are relatively expressed to the values in the case of $\tau_h=0$ and are displayed by open and closed circles and triangle marks, respectively. Suffix "4" shows the value at No. 4, the end in the moving direction, and suffix "18" at No. 18, the opposite end. According to the increase of ε, both amplitudes of crest and trough increase with the same rate in the moving direction and decrease in the opposite direction. The energy varies more strongly. As the amplitude increases, the period becomes shorter, therefore the energy is not proportional to the square of the amplitude but there is the relation of $E_d \propto A_c^{1.36}$.

The directivity coefficient D is defined by the ratio of the value of the wave radiated toward the moving direction to the one toward the opposite direction. The open and closed circles in Fig. 9 are the directivity coefficient for a crest amplitude, $D_c(0)$, and the one for a half period, $D_p(0)$, which are displayed with respect to ε where the curves shown by the solid lines are the theoretical results for the one-dimensional model by *Homma* [1952], which are $(1+\varepsilon)/(1-\varepsilon)$ for the amplitude and a reciprocal of that for the period.

In the present experiment for the two-dimensional model, $D_c(0)$ is larger than Homma's result and is fairly well approximated by the curve of $(1+\sqrt{2}\varepsilon)/(1-\sqrt{2}\varepsilon)$ which is shown by a broken line in the figure. $D_p(0)$ is not so different from the value of one-dimensional model and the discrepancy between both models is about 10% for $\varepsilon=0.35$. The directivity coefficient is the function of the azimuth θ which is the angle between a certain direction and the moving direction of bottom deformation. Fig. 10 shows the variation of the directivity coefficient $D_c(\theta)$ and $D_p(\theta)$ with respect to θ, for various values of τ_h. The directivity coefficient $D_c(\theta)$ can be approximated by the curve of $1+K\cos\theta$. As $1+K$ is $D_c(0)$ which is the directivity coefficient in the case of $\theta=0°$, it follows,

$$D_c(\theta)=1+\{D_c(0)-1\}\cos\theta, \tag{1}$$

where

$$D_c(0)=(1+\sqrt{2}\varepsilon)/(1-\sqrt{2}\varepsilon). \tag{2}$$

$D_p(\theta)$ is also approximated by the curve of $1-K'\cos\theta$. As $1-K'$ is

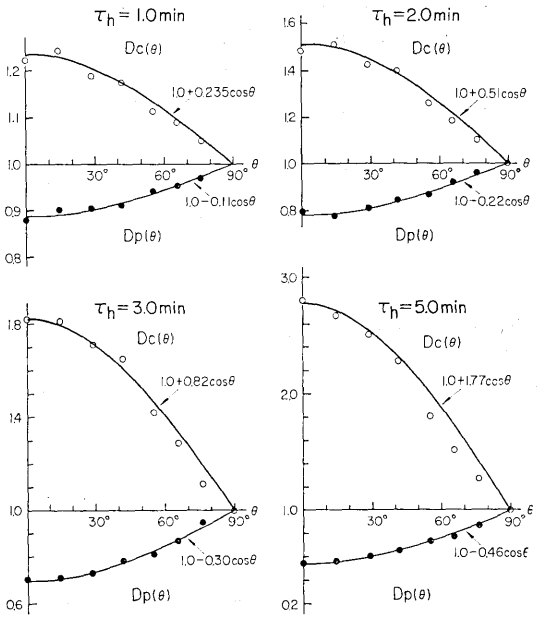

Fig. 10. Variation of the directivity coefficient with respect to an azimuth θ.

$D_p(0)$, $D_p(\theta)$ is expressed by the equation similar to (1), provided the suffix p is substituted for c, and

$$D_p(0) \fallingdotseq (1-\varepsilon)/(1+\varepsilon). \tag{3}$$

4d. Wave energy

The total energy of the waves radiated outward from the deformed area, in the condition $\tau_v=1.5$ min and $\tau_h=0.0$ min, becomes 1.55×10^{20} ergs. On the other hand, if the bottom deformation was instantaneously performed, the generated wave energy can be calculated to be 2.03×10^{20} ergs as the potential energy of sea surface elevation which is equal to the upheaval of the sea bottom. Thus, the former corresponds to 0.76 times the latter. The decrease of wave energy in the former case can be attributed to the finite speed of the vertical bottom deformation. The ratio of wave amplitude at the center of deformed area becomes 0.91, its squared value being 0.825, which is fairly close to the degree of the energy deduction.

In the case when the bottom deformation moves horizontally, the total energy of radiated waves is calculated to be 1.63×10^{20}, 1.76×10^{20} and 3.03×10^{20} ergs for $\varepsilon=0.21$, 0.35 and 0.7, respectively. These values are 1.05, 1.14 and 1.95 times that in the case of $\varepsilon=0$, increasing remarkably, as the horizontal speed of the bottom deformation approaches

the long-wave velocity. They can be expressed by the relation $E/E_0=1/(1-\varepsilon^2)$, being analogous to the general theory for the surface elevation ζ excited by a travelling atmospheric disturbance, in which the relation $\zeta/\zeta_0=1/\sqrt{1-\varepsilon^2}$ is given for the case of two-dimensional propagation with the suffix "0" indicating the case when the disturbance does not travel. The present fact, therefore, shows apparently the effect of coupling between the excited wave and the horizontal movement of bottom deformation.

5. Moving deformation on the sloping bottom

Most tsunamis take place in the region of a continental slope. It is considered that the directivity due to the movement of the bottom deformation would be modified by the presence of slope. Suppose the sea bottom profile, as shown in Fig. 11, along the moving direction of deformation.

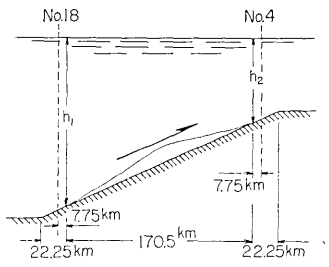

Fig. 11. Assumed profile of a sloped bottom.

The conditions of the computation in this case are $\tau_v=1.5$ min, $\tau_h=3$ min, with the same shape of sea bottom deformation as in the preceding section. The bottom slope is given in the following table.

Table 2.

h_1	h_2	slope; S
4000m	3000m	$1\times1/170.5$
〃	2000	2
〃	1000	3
2000	4000	-2

If the sea becomes shallow in the same direction as the movement of the bottom deformation, the increase of amplitude with shoaling is further strengthened by the shortening effect of period due to the movement of the bottom deformation. However, in the opposite case, the effect of the moving deformation and the effect of slope cancel each other. This is understood from the wave form in Fig. 12.

The amplitudes of crest and trough at points Nos. 4 and 18 vary due to the bottom slope as shown in Fig. 13, where values are shown as the ratios to the values in the case of uniform depth. The increase of the crest amplitude is not so remarkable even for the slope of 2/170,

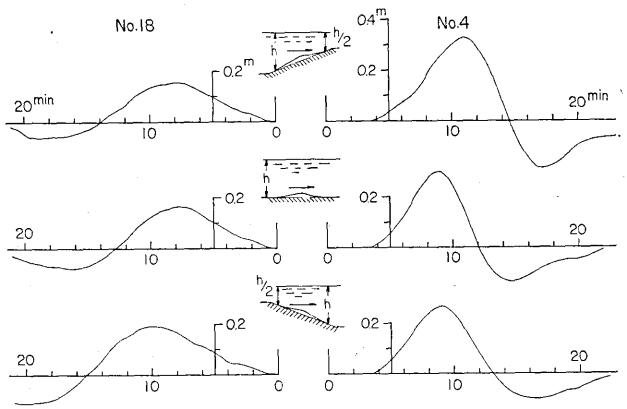

Fig. 12. Typical wave forms radiated in opposite directions of deformed area on the sloping bottom.

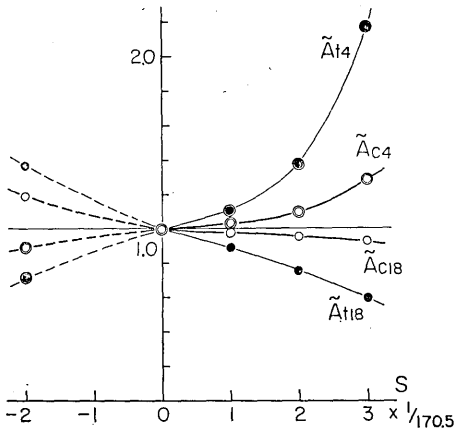

Fig. 13. Variation of amplitudes of a crest and a trough with respect to a slope.
A_c: an amplitude of crest.
A_t: an amplitude of trough.

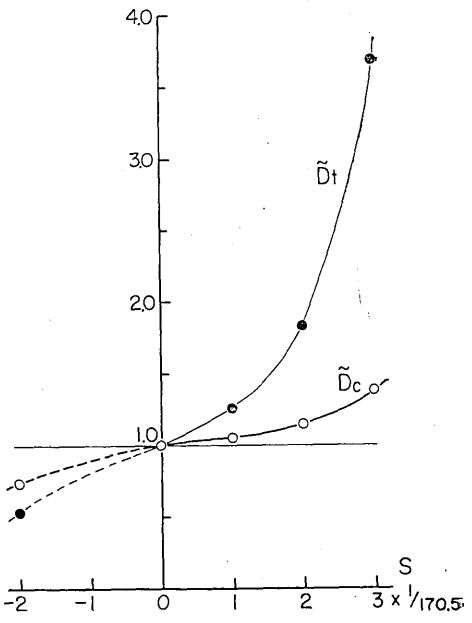

Fig. 14. Variation of directivity coefficient with respect to a slope.
D_c: a directivity of crest amplitude.
D_t: a directivity of trough amplitude.

but the amplitude of trough in the slope of 2/170 becomes 1.4 times that in a uniform depth and reaches 2.2 times, for the slope of 3/170.

The variation of directivity attributed to the slope is expressed by

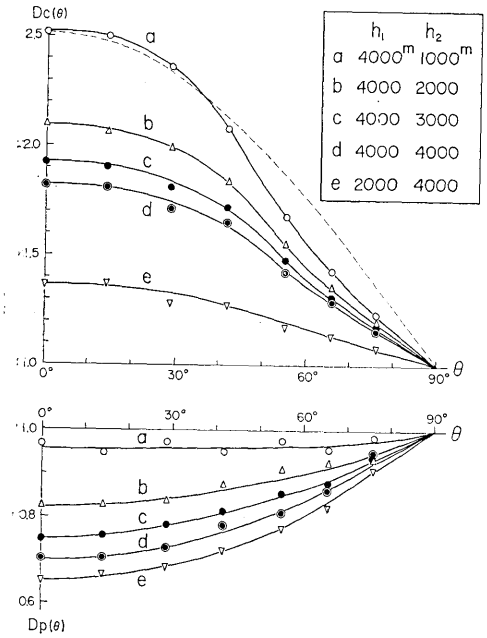

Fig. 15. Variation of directivity coefficient with respect to an azimuth θ, in a sloping bottom.

the ratio to that in a uniform depth, as shown in Fig. 14. As mentioned in the preceding section, the discrepancy between the directivity for a crest and for a trough was hardly recognized in the case of uniform depth. In contrast, it is remarkable that the directivity in the presence of the slope is quite different for a crest and a trough.

The relation of the directivity coefficient with the azimuth θ becomes as shown in Fig. 15, where the upper figure is the one for the amplitude of crest and the lower figure for the period. Comparing with the curve, $1+K\cos\theta$ (broken line), which was deduced in the preceding section, considerably low values are seen in $\theta=50°$ to $80°$. This seems to be the effect of a wave refraction on a sloping bottom.

6. Consideration of a practical application

Aki [1967] stated in the summarized paper of earthquake mechanism that the rupture velocity was 2 to 3 km/s. Therefore, the sea bottom deformation, which is an appearance of a fracture zone on the earth's surface, will perhaps move with a comparable velocity.

On the other hand, the epicenters of tsunamigenic earthquakes near Japan are located at places where the water depth is 100 to 200 m in the Japan Sea and 1000 to 4000 m in the Pacific Ocean area. Consequently, long-wave velocities are 31 to 45 m/s and 100 to 200 m/s, respectively. Suppose the rupture velocity is 2 km/s, ε is equal to 0.015 to 0.023 and 0.05 to 0.1, respectively. Taking into account the directivity coefficient as shown in Fig. 9, the effect due to the moving source is negligible when the tsunami takes place in the shallow sea bottom of the Japan Sea. In the case when the source is located in the deep sea such as the Pacific Ocean side, the directivity is about 1.15 to 1.32.

The observation of tsunami in the open sea has not been performed yet, so that the separation of effect due to a sloping bottom is very

difficult in an actual case.

The difference of the arrival time, as shown in Fig. 6, may be applicable for the determination of the speed and direction of the moving bottom deformation when many observations surrounding the source area were obtained.

7. Acknowledgment

The author would like to acknowledge the useful advice and encouragement of Professor K. Kajiura, and the assistance of Mr. M. Koyama with the diagrams.

The numerical calculation was carried out on an IBM 360/40 at the Earthquake Prediction Observation Center, Earthquake Research Institute.

References

AIDA, I., 1969, Numerical experiments for the tsunami propagation—the 1964 Niigata tsunami and the 1968 Tokachi-oki tsunami, *Bull. Earthq. Res. Inst.*, **47**, 673-700.

AKI, K., 1967, Studies of earthquake mechanism by use of surface waves, *Zisin* [ii], **20**, No. 4, Special Issue, 65-68, (in Japanese).

BEN-MENAHEM, A. and M. N. TOKSÖZ, 1962, Source-mechanism from spectra of long-period seismic surface-waves, 1. The Mongolian Earthquake of December 4, 1957, *Jour. Geophys. Res.*, **67**, 1943-1955.

HIRASAWA, T., 1965, Source mechanism of the Niigata Earthquake of June 16, 1964 as derived from body waves, *Jour. Phys. Earth*, **13**, 35-66.

HOMMA, S., 1950, Waves generated by the progress of submarine change (I), *Quarterly Jour. Seism.*, **14**, No. 3-4, 65-69, (in Japanese).

HOMMA, S., 1952a, Waves generated by the progress of submarine change (II), *Quarterly Jour. Seism.*, **16**, No. 1, 81-87, (in Japanese).

HOMMA, S., 1952b, Waves generated by progressing deformation of the sea bottom (III), *Quarterly Jour. Seism.*, **16**, No. 3-4, 23-63, (in Japanese).

ICHIYE, T., 1950, On the wave caused by the disturbance travelling at the bottom (I), *Mem. Kobe Mar. Obs.*, **8**, 12-18.

ICHIYE, T., 1951, On the wave caused by the disturbance travelling at the bottom (II), *Mem. Kobe Mar. Obs.*, **9**, 23-24.

KAJIURA, K., 1966, Tsunami, *Hydro Technique Series 66-13, Committee on Hydraulics, JSCE*, 1-22, (in Japanese).

NAKAMURA, K., 1953, On the waves caused by the deformation of the bottom of the sea, I, *Sci. Rep. Tohoku Univ. Ser. 5, Geophys.*, **5**, 167-176.

TAKAHASI, R., 1942, On seismic sea waves caused by deformations of the sea bottom, *Bull. Earthq. Res. Inst.*, **20**, 375-400.

TAKAHASI, R., 1945, On seismic sea waves caused by deformations of the sea bottom, Second report, *Bull. Earthq. Res. Inst.*, **23**, 23-35.

38. 進行する海底変動によって生ずる津波の数値実験

地震研究所　相田　勇

海底変動が水平に進行する場合に，海面上に生ずる津波について数値実験を行い，その性質を検べた．

変動域の平面形状は円形で，その1つの直径の方向に変動が進行し，最終的に垂直変動の大きさが $\eta=\exp(-r^2/a^2)$ であらわされるようなモデルを与えた．変動の進行と同じ方向に射出される波の振幅と反対方向に射出される波の振幅の比 $D(0)$ は，$D(0)=(1+\sqrt{2}\varepsilon)/(1-\sqrt{2}\varepsilon)$ によってあらわされることがわかった．ここに ε は長波速度と変動の進行速度の比である．この結果は一次元伝播の場合の理論的な値よりやや大きい値を示す．又変動の進行方向と θ の角度をなす方向に対しては，

$$D(\theta)=1+\{D(0)-1\}\cos\theta$$

であらわされる．

又海底変動が，傾斜面に起る場合については，変動の進行方向に水深が浅くなっていると，前述の D の値は一層大きくなる．